ISSN: 2447-3359

REVISTA DE GEOCIÊNCIAS DO NORDESTE

Northeast Geosciences Journal

v. 10, nº 1 (2024)

https://doi.org/10.21680/2447-3359.2024v10n1ID34833

Computational modeling of percolation flow in an earthen dam: a comparison of 2d and 3d flow models

Modelagem computacional do fluxo de percolação em barragem de terra: um comparativo entre modelo 2D e 3D

Maísa de Calda Lopes[1]; Luiz Gustavo Menezes Morgado[2]; Gustavo Hugo Pereira Vidal[3]; Luiz Alberto Ribeiro Mendonça[4]; Marco Aurélio Holanda de Casto[5]

[1] Federal University of Ceará, Department of hydraulic and environmental engineering, Fortaleza-CE, Brasil. Address: maisa.lopes@alu.ufc.br
ORCID: https://orcid.org/0009-0009-4950-828X

[2] Federal University of Ceará, Civil Engineering Course, Fortaleza-CE, Brasil. Address: luizmorgado@alu.ufc.br
ORCID: https://orcid.org/0009-0005-0393-1876

[3] Federal University of Ceará, Civil Engineering Course, Fortaleza-CE, Brasil. Address: gustavo.hugo@aluno.ufca.edu.br
ORCID: https://orcid.org/0009-0005-8055-1332

[4] Federal University, Civil Engineering Course, Juazeiro do Norte-CE, Brasil. Address luiz.alberto@ufca.edu.br
ORCID: https://orcid.org/0000-0002-8166-3337

[5] Federal University of Ceará, Department of hydraulic and environmental engineering, Fortaleza-CE, Brasil. Address: marco@ufc.br
ORCID: https://orcid.org/0000-0001-5134-7213

Abstract: In this study, simulations of flows in the dam body and foundation of the Olho d'Água dam (built in the Brazilian semi-arid region and monitored by the Water Resources Management Company of the State of Ceará - COGERH) were analyzed. The analysis utilized a 2D stationary flow model, employing the SEEP/W application (with solutions obtained through the finite element method), and a 3D transient flow model, using the MODFLOW application (with solutions obtained through the finite difference method). The results indicated that the 3D transient modeling provides more accurate outcomes and could be a valuable tool in understanding the dynamics of seepage flow in earth dams. Additionally, there is potential for implementing the MODFLOW application as a tool for monitoring and analyzing seepage flow in earth dams, offering critical insights that could prevent failures and optimize water resource management. These advancements are crucial for the design, monitoring, and management of dams, especially in the challenging context of Northeast Brazil, where earth dams are prevalent.

Keywords: Percolation flow; Earthen dam; Computational modeling.

Resumo: Neste trabalho foram analisadas simulações de fluxos no maciço e na Foundation da barragem Olho d'Água (construída no semiárido brasileiro e monitorada pela Companhia de Gestão dos Recursos Hídricos do Estado do Ceará - COGERH), utilizando o modelo de fluxo 2D estacionário, a partir do aplicativo SEEP/W (com soluções obtidas através do método dos elementos finitos) e o modelo de fluxo 3D transiente, a partir do aplicativo MODFLOW (com soluções obtidas através do método das diferenças finitas). Os resultados mostraram que a modelagem 3D transiente fornece resultados mais precisos, podendo ser uma ferramenta a ser utilizada no entendimento da dinâmica do fluxo percolado em barragens de terra. Soma-se ainda, a possibilidade de implementação do aplicativo MODFLOW como instrumento de monitoramento e análise de fluxo de percolação em barragens de terra, oferecendo *insights* críticos que podem prevenir falhas e otimizar a gestão de recursos hídricos. Estes avanços são essenciais para o dimensionamento, monitoramento e gestão de barragens, especialmente no contexto desafiador do Nordeste brasileiro, onde as barragens de terra são prevalentes.

Palavras-chave: Fluxo de percolação; Modelagem computacional; Barragem de terra.

Received: 12/12/2023; Accepted: 06/12/2024; Published: 04/03/2024.

1. Introduction

Concerns regarding issues related to the hydraulic stability of earth dams have led many researchers to apply porous media flow models, as well as to formulate numerical models that solve differential equations describing the flow of water percolation in porous media. The transient water flow through the body and foundation of earth dams, subjected to a natural hydraulic gradient, is described by partial differential equations governing water percolation in free or confined aquifers in a three-dimensional domain consisting of heterogeneous and anisotropic material. However, the design and analyses required for the development of an executive project for dams are carried out using a 2D domain. According to Freeze and Cherry (1979), this is accomplished through flow networks, considering a 2D cross-sectional area consisting of homogeneous and isotropic material selected within the three-dimensional (3D) domain. However, recent studies have shown that this methodology can lead to problems. According to Nazari (2018), the simplifications used in 2D modeling of groundwater flow can result in inadequate solutions. Bayat et al. (2019) argue that the hydraulic behavior of percolation in both the foundation and the body cannot be accurately predicted using conventional methods (2D and stationary analysis).

Chen and Zhang (2006) and Pimenta et al. (2020) reported that failures in dam drainage systems commonly begin with resurgences and erosions on the abutments. This situation is not observed in conventional simulations (Bayat et al., 2019), which, being overly simplified, often underestimate percolation flow and the risk of failure at the abutment boundaries. However, it can be analyzed in a 3D modeling approach. According to Lópes and Promotor (2016), 3D modeling allows the inclusion of irregular geometries of the structure, topographic configuration of the soil, unsaturated flow conditions, and more realistic boundary conditions. Furthermore, as stated by Rocha et al. (2023), 3D simulations enable a more precise understanding of hydraulic phenomena, providing valuable information for the design, analysis, and management of hydraulic structures, thereby reducing the risks associated with corrective measures throughout the operational lifespan of the unit.

Some researchers, such as Chen and Zhang (2006) and Kacimov et al. (2019), conducted comparative studies between 2D and 3D modeling regarding percolation flow in the body and foundation of dams. However, these studies were carried out under steady-state conditions, considering hydrodynamic equilibrium, and neglecting the effects of specific storage coefficient and specific discharge.

According to Bayat et al. (2019), factors such as material availability, construction speed, and economic aspects make earth dams the preferred choice. The analysis of percolation flow must be even more meticulous in earth dams, as the water flow through the dam body and foundation is used for the design of internal drainage systems. According to Terzaghi and Peck (1962), it is advisable in earth dams to minimize the percolation of water from the reservoir through the dam body to its core, preventing regressive erosion through a vertical sand drain, in conjunction with a horizontal drain or a drainage mat composed of gravel and sand. This is complemented by a toe drain, also consisting of gravel and sand.

The National Policy on Dam Safety, established by Law No. 14,066, dated September 30, 2020, mandates that the safety of a dam must be considered in all phases of its existence: design, construction, and operation (BRAZIL, 2020). In the design phase, both the sizing and the adopted simplifications are highlighted. During the construction phase, emphasis is placed on compliance with the criteria established in the executive project. In the operation phase, attention is focused on the continuous monitoring of the structure.

In the Brazilian Northeast, as indicated by Moreira et al. (2019), the abundant presence of soils suitable for construction has led to the prevalence of earth dams. Due to a pattern of rainfall equal to or less than 800 mm annually, the semi-arid region often experiences years of drought, resulting in water scarcity for human and animal consumption, as well as for various productive activities (ALVES, LIMA; 2020). To address this issue, there has been governmental encouragement for the construction of numerous dams (SANTOS et al., 2014).

This study aims to analyze the percolation flow in an earth dam, focusing on the Olho D'Água dam located in the municipality of Várzea Alegre, Ceará, Brazil. To achieve this, a 2D steady-state flow model was employed using the SEEP/W application and a transient 3D model was developed using the MODFLOW application. The investigation seeks to explore the hypothesis that transient 3D modeling of percolation flow in earth dams provides more accurate and representative results compared to stationary 2D analyses. This considers the three-dimensional and transient nature of fluid mechanics in these structures. Furthermore, the study aims to establish the MODFLOW application not only as an effective tool for analyzing percolation flow in dams but also as an instrument for the continuous monitoring of earth dams.

2. Study Area

The Olho d'Água dam, located in the northeastern semi-arid region (Figure 1), stands at a height of 24 meters with a storage capacity of 21 million cubic meters and a hydraulic basin covering 456 hectares. Figure 2 provides an overview of the dam body.

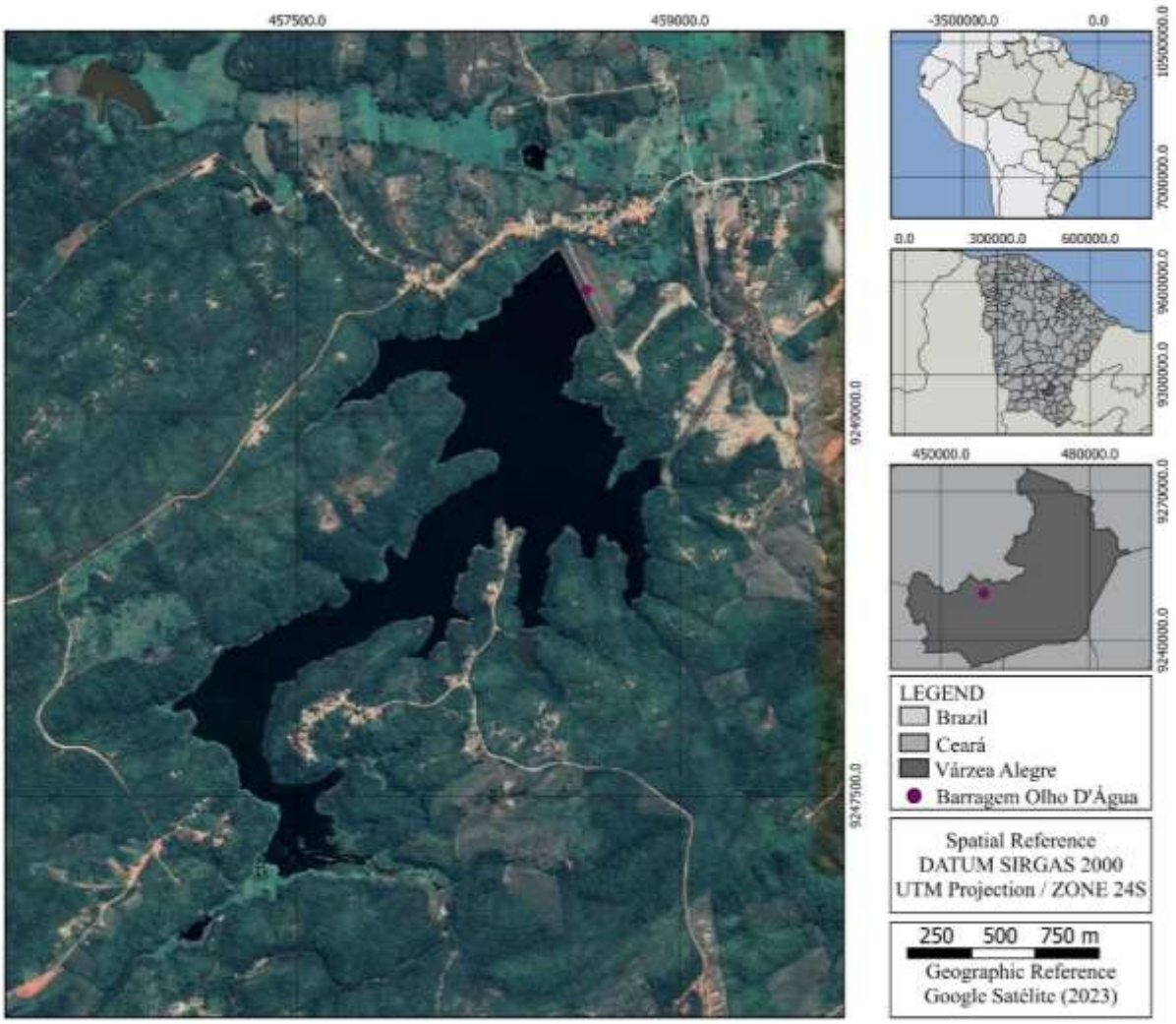

Figure 1 – Location map
Source: Authors (2023)

Figure 2 – General view of the dam.
Source: http://portal.cogerh.com.br

The executive project for the Olho d'Água dam was developed by the company Aguasolos - Consultora de Engenharia Ltda (SRH, 1988a) and executed by the 3rd Construction Engineering Battalion of the Army, being inaugurated in 1998. However, during the construction, unforeseen changes took place that were not accounted for in the executive project and were not documented in an as-built project. These changes are described in the Instrumentation Diagnostic Report (COGERH, 2021).

According to SRH (1988a), the dam was designed as a zoned type with a core consisting of sandy-silt-clay soils SC-SM (according to the SUCS classification) and flanks made of low-plasticity clay CL. It features a crest width of 6 m, upstream and downstream slope inclinations of 1:3.0 (V:H) and 1:2.6, respectively. The upstream impermeable blanket spans 120 m, with a sealing trench of 46 m in width, a compacted embankment bench of 70 m, and an internal drainage system consisting of horizontal and vertical filters (Figure 3a).

However, with the changes made during the execution phase, the dam became a homogeneous type consisting of SC-SM soils. It now has an upstream impermeable blanket of 18 m, without a compacted embankment bench downstream, and with a reduced internal drainage system (Figure 3b). After construction, issues related to artesian pressure in the foundation arose, leading to the installation of relief wells downstream (Figure 3b).

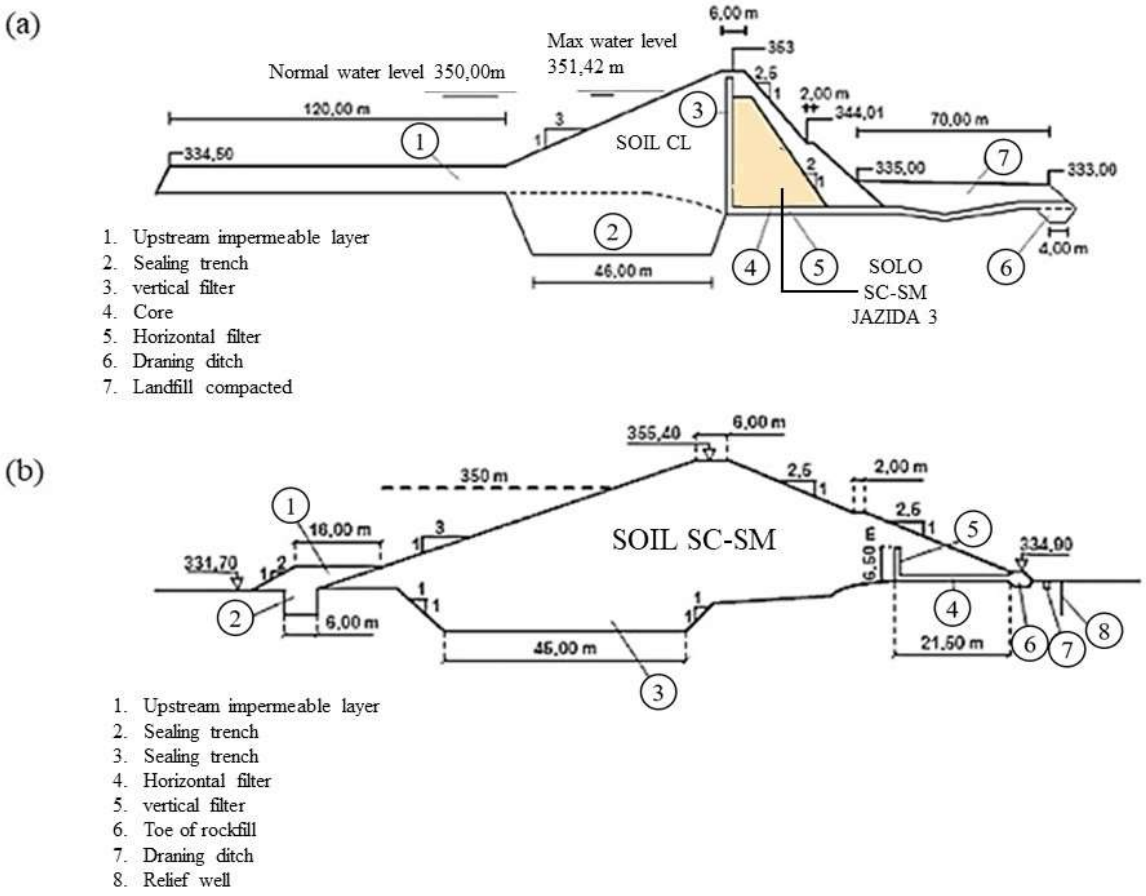

Figure 3 – Maximum section of the executive project (a) and executed maximum section (b)
Source: Modified from Dantas Neto and Carneiro (2013, cited in Araújo, 2013)

3. Water percolation in soil

The flow that percolates through the dam body and foundation of earth dams is described by equations governing the percolation of water in porous media. The MODFLOW application considers the cells of the discretized domain below the cells containing the water table (Figure 4a and Equation 1) as confined (Figure 4b and Equation 2).

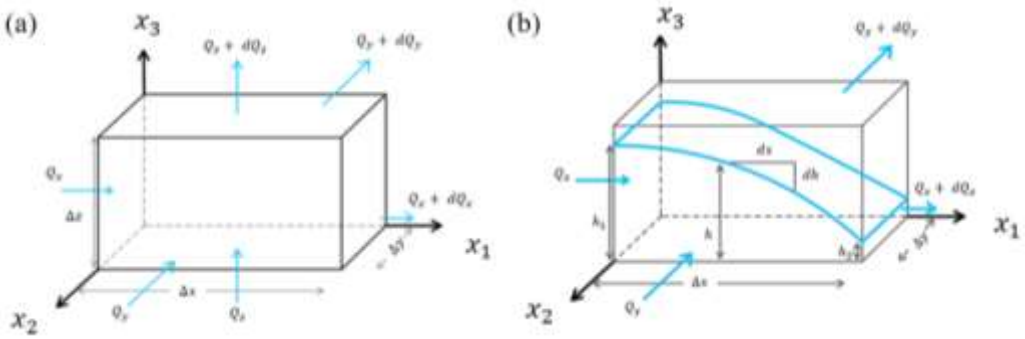

Figure 4 - Prismatic control volume for confined (a) and unconfined (b) aquifer
Source: Authors (2023)

[1] $$\sum_{i=1}^{3} \frac{\partial}{\partial x_i}\left(k_{ii}\frac{\partial h}{\partial x_i}\right) \pm q_s = S_S\frac{\partial h}{\partial t}$$

[2] $$\sum_{i=1}^{2} \frac{\partial}{\partial x_i}\left(hk_{ii}\frac{\partial h}{\partial x_i}\right) \pm q = S_y\frac{\partial h}{\partial t}$$

Em que:
k_{ii}: principal component of the hydraulic conductivity tensor [LT-1];
h: hydraulic head [L];
q_s: external flow per unit volume representing a source or sink [T-1];
SS: specific storage coefficient of porous material [L-1];
q: external flow per unit area of the cross-sectional area representing a source or sink [LT-1];
Sy: specific yield [-].

Considering the confined situation, the 3D domain is confined at the top and bottom by relatively impermeable materials, and the variation in water volume is given by the specific storage coefficient (SS), defined based on the compressibilities of the porous medium and water. The water table within the 3D domain is subjected to atmospheric pressure, and the flow occurs under the influence of gravity, with the variation in water volume given by specific yield (Sy) (Freeze and Cherry, 1979). In the derivation of Equation 2, the Dupuit-Forchheimer simplification was applied, assuming predominantly horizontal flow with specific discharge Q only in the x1 and x2 directions.

In steady 2D flow, Equations 1 and 2 are simplified by neglecting terms not aligned with the coordinate containing the cross-sectional area defining the domain. Additionally, the second term representing the temporal variation of the hydraulic head is disregarded.

The solutions to Equations 1 and 2, as well as their simplifications, are obtained through numerical methods. Commonly used methods include the Finite Element Method (FEM) and the Finite Difference Method (FDM).

The MEF provides a numerical solution for an initial boundary value problem (PASHAH, 2023). The basic idea is to discretize the region of the continuous solution into a group of finite elements connected in a certain way (XU et al. 2022), where, according to Xu and Huo (2020), its solution is based on the variational principle and the method of weighted residuals. The FDM is a domain discretization technique that converts the governing problem into a difference equation. Functional values are approximated at the nodes of the grid. The advantage of the numerical approach in this study is that minimal iterations are required to achieve optimal accuracy at each time step (HUSSAIN, ALI; 2023).

A decision on which method to apply depends on the user, considering its ease of use and the program in which it will be implemented. For example, SEEP/W (GEO-SLOPE, 2001) is a graphical program owned by GEO-SLOPE International Ltd., operating on Microsoft Windows. Modeling is carried out using the FEM for porous media flow, both in steady-state and transient conditions, for saturated and unsaturated soils. On the other hand, MODFLOW (MCDONALD, HARBAUGH; 1988), a modular three-dimensional finite difference groundwater flow model, is one of the most well-known programs used in 3D simulation of subsurface flows and contaminant transport, employing the FDM.

4. Methodology

Steady 2D flow simulations were conducted using the SEEP/W application, version 2018, while transient 3D flow simulations were carried out using Visual MODFLOW, version 2011.1. In both programs, Equations 1 and 2 are appropriately applied to each cell in the mesh of the discretized domain. Internal flow is determined by Darcy's Law, and external flow is governed by boundary conditions that define functions formulating terms representing sources and/or sinks.

4.1 Information used in the construction of the 3D conceptual hydrogeological model and transient model

In the MODFLOW application, the model domain was defined as a rectangular prism with dimensions of 210 m x 228 m x 52 m, discretized in a finite difference mesh with 228 rows, 214 columns, and 59 layers. Different types of materials, hydrogeological properties of the porous medium (k, SS, and Sy), instrumentation (piezometers, PZ, and water level meters, NA), as well as initial and boundary conditions were incorporated into the model, as described below.

- **Stratified profile**

The stratigraphic profiles of the embakment and foundation, as well as the details of the boreholes, were obtained from the executive project (SRH, 1988c). The foundation characterization, based on geotechnical studies conducted through auger, pick, percussion, and mixed borehole methods, identified a thick alluvium deposited over the decomposed crystalline basement. It consists of eight layers of different materials (Figure 4).

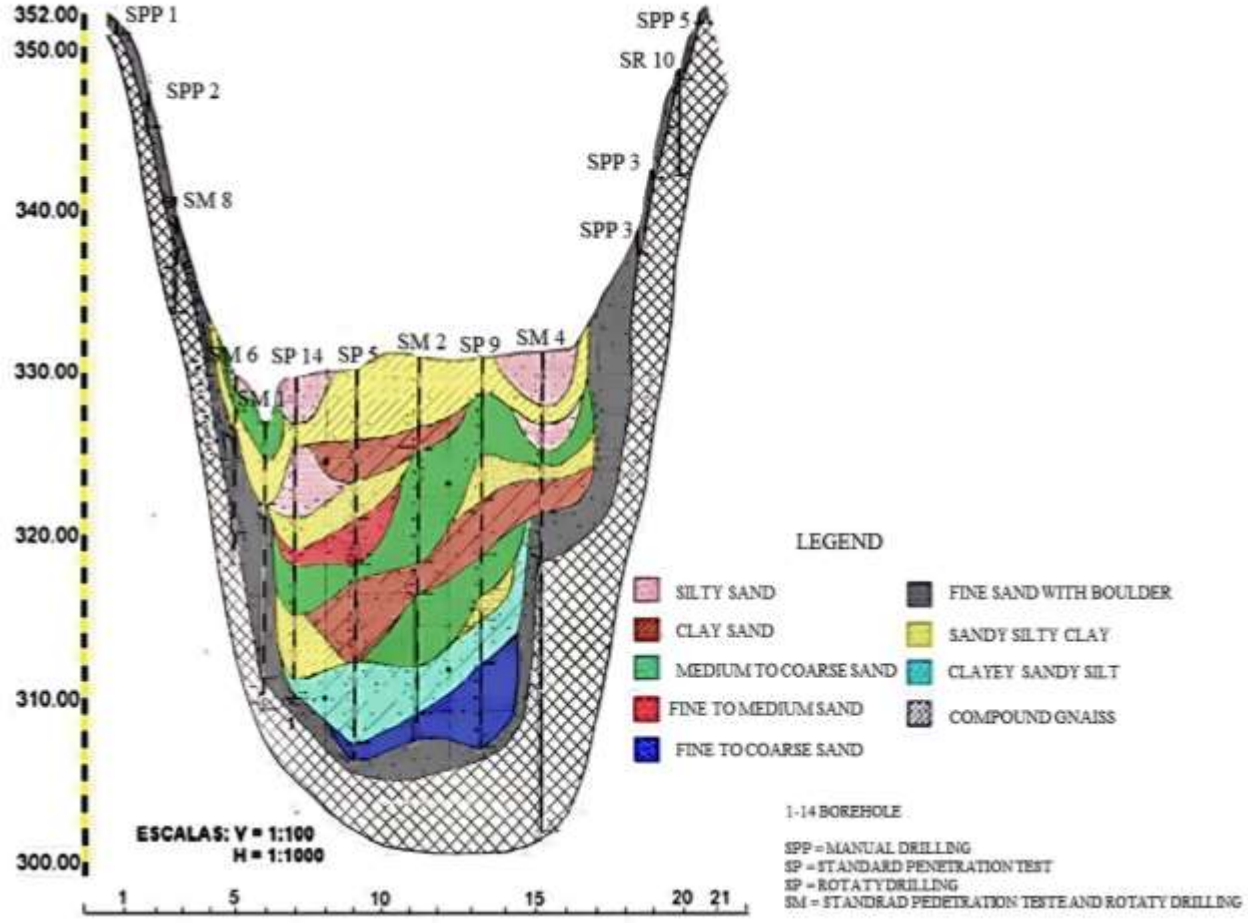

Figure 4 – Stratified profile of the foundation obtained based on borehole results, Source: Adapted from SRH (1988b)

- **Topographic and bedrock surfaces**

To obtain the topographic surface, the adjustment of the sections provided in the executive project (SRH, 1988c) was performed, and georeferencing was used to obtain the coordinates of points describing the mass and the riverbed upstream and downstream. Subsequently, the topography was obtained through kriging of topographic points using the SURFER application version 23. For the construction of the bedrock surface, the rock boundary presented in the stratified profile (Figure 4) was considered, and the points were obtained through georeferencing and kriging.

- **Hydrogeological properties**

With information on each type of soil present in the foundation (Figure 4) and the material used for dam construction (Araújo, 2013), literature was consulted to obtain ranges of values for hydrogeological properties k (Chapuis and Aubertin (2003)), SS (Germain et al. (2020)), and Sy (Johnson (1967)). From these ranges, values for k were obtained for use in the initial sensitivity analysis of the model in steady-state, and for SS and Sy in the transient regime (Table 1). The layers constituting the homogeneous mass were considered anisotropic (kx33 = 10-1 k, with k = kx11 = kx22) (Fell et al. 1992), while the others were considered isotropic (kx11 = kx22 = kx33).

Table 1 – Hydrogeological properties used at the beginning of the analysis

Material	Location	k(m/s)	S_S (1/m)	S_y (-)
Silty-clayey-sand	Dam body	10^{-4}	5×10^{-3}	$3{,}0 \times 10^{-2}$
Silty sand	Foundation	10^{-3}	5×10^{-3}	$2{,}5 \times 10^{-1}$
Clayey sand	Foundation	10^{-4}	5×10^{-3}	$2{,}5 \times 10^{-1}$
Medium to coarse sand	Foundation	10^{-3}	5×10^{-3}	$2{,}5 \times 10^{-1}$
Fine to medium sand	Foundation	10^{-3}	5×10^{-3}	$2{,}5 \times 10^{-1}$
Fine to coarse sand	Foundation	10^{-3}	5×10^{-3}	$2{,}5 \times 10^{-1}$
Fine sand with gravel	Foundation	10^{-3}	5×10^{-3}	$1{,}6 \times 10^{-1}$
Silty sandy clay	Foundation	10^{-6}	5×10^{-3}	$2{,}5 \times 10^{-1}$
Silty sandy clayey	Foundation	10^{-7}	5×10^{-3}	$3{,}0 \times 10^{-2}$
Crushed stone	Rip-rap	10^{-3}	5×10^{-3}	$2{,}2 \times 10^{-1}$
Crushed stone	Rock toe	10^{-2}	5×10^{-3}	$2{,}2 \times 10^{-1}$

Source: Authors (2023)

- **Discretization of the dam body and foudantion**

Figure 5 depicts the discretization of the maximum cross-sectional area (corresponding to borehole SP-9 shown in Figure 3), along with three longitudinal sections: one upstream (section AA), one at the centerline of the dam body (section BB), and one downstream (section CC).

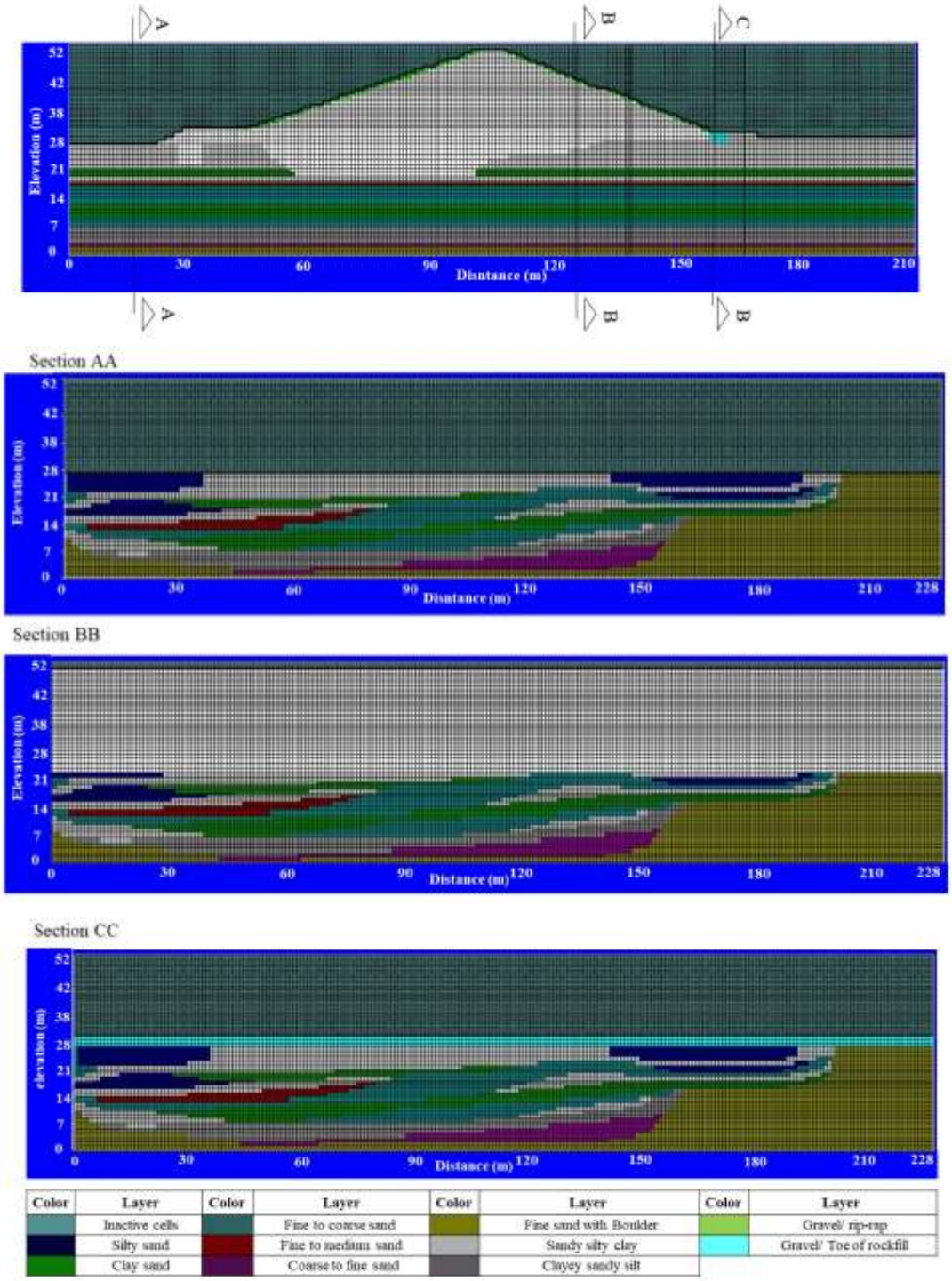

Color	Layer	Color	Layer	Color	Layer	Color	Layer
	Inactive cells		Fine to coarse sand		Fine sand with Boulder		Gravel/ rip-rap
	Silty sand		Fine to medium sand		Sandy silty clay		Gravel/ Toe of rockfill
	Clay sand		Coarse to fine sand		Clayey sandy silt		

Figura 5 – Discretization of the maximum cross-section and longitudinal sections
Source: Authors (2023)

- **Hydraulic head**

The observed hydraulic head values used in model calibration were obtained from readings of instruments installed in the dam body (NA) and in the foundation (PZ). The instruments were placed in three cross-sectional sections: instrumented section 01, passing through borehole 09; 02, through 02; and 03, through 05 (Figure 6). In total, there were 21 instruments, comprising 8 NA and 13 PZ.

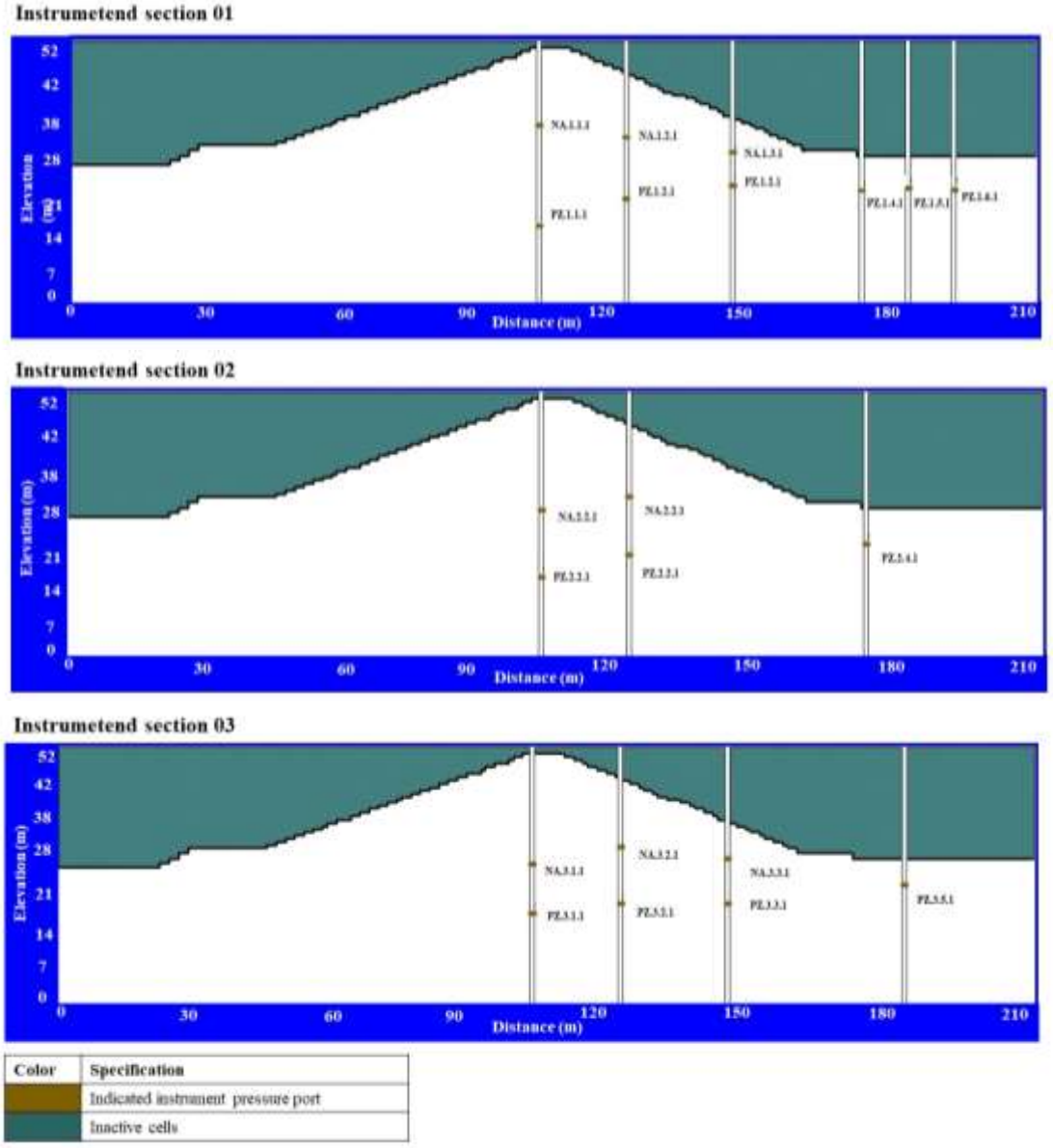

Figure 6 – instrumenteds sections
Source: Authors (2023)

- **Boundary conditions**

The boundary conditions assigned to the conceptual hydrogeological model were of the following types:Dirichlet, defined by constant hydraulic head values specified at the upstream and downstream boundaries of the dam body, representing the stored water in the reservoir at different levels and the spring discharges, respectively;Neumann, defined by no-flow regions (inactive cells) representing impermeable boundaries delimiting the model domain;Cauchy, defined by drains representing the internal drainage system and relief wells installed downstream of the dam body.Figure 7 shows the representation of boundary conditions in the maximum cross-sectional area, highlighting the internal drainage system and relief well.

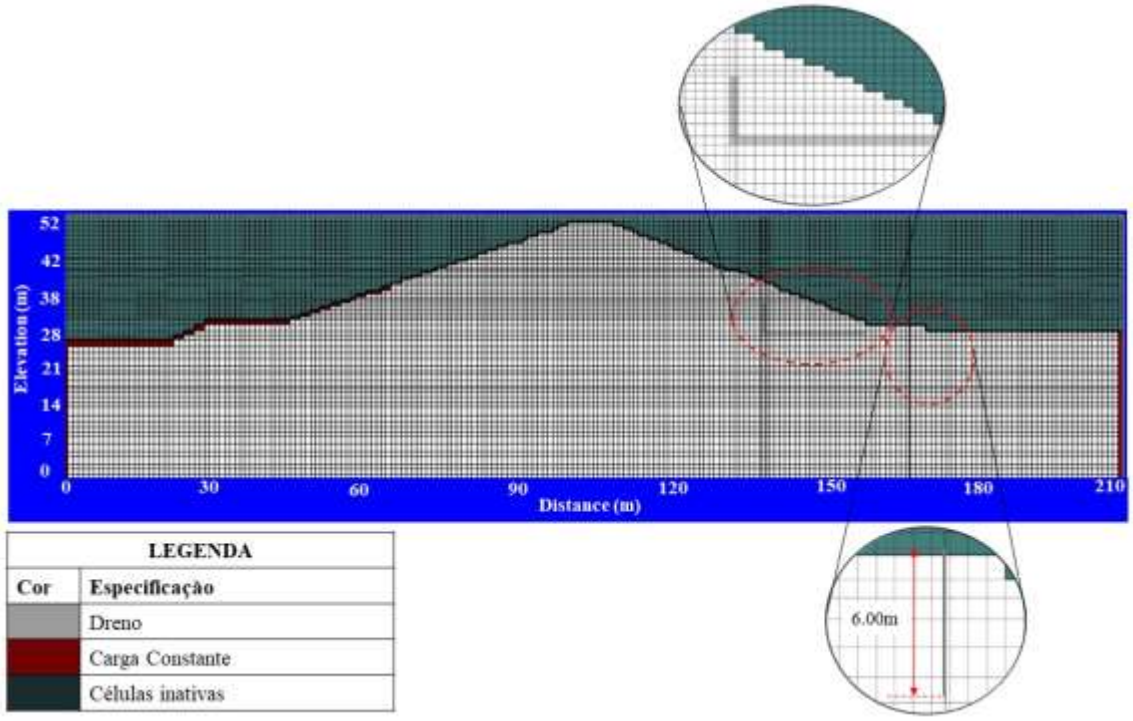

Figure 7 – Representation of boundary conditions
Source: Authors (2023)

The equation determining the flow extracted by the drains in each cell containing them is defined as a function of conductance and the difference between the hydraulic head specified in the drain and the hydraulic head calculated by the model. Since there is no formulation for obtaining conductance, it was adjusted during the model calibration, with initial values provided as 0.5, 1.0, 1.5, and 2.0 m²/day for the horizontal and vertical filters and relief wells, respectively.

4.2 Informations used in the construction of the conceptual 2d and steady-state hydrogeological model

In the SEEP/W application, the model domain was defined considering the maximum cross-sectional area of the dam body (Figure 3b) and the four superficial layers of the foundation identified in borehole SP-9 (Figure 4). The domain was discretized into a finite element mesh consisting of quadrilaterals and triangles with a global size of 2.0 m in the region of the dam body and foundation, refined to 0.5 m in the regions of the filters, toe riprap, and relief well.

Figure 8a shows the discretized domain, the constituent materials, the constant head boundary conditions located upstream and downstream, and the location of instruments used to obtain calculated hydraulic heads. Meanwhile, Figure 8b displays the finite element mesh used in the analyses.

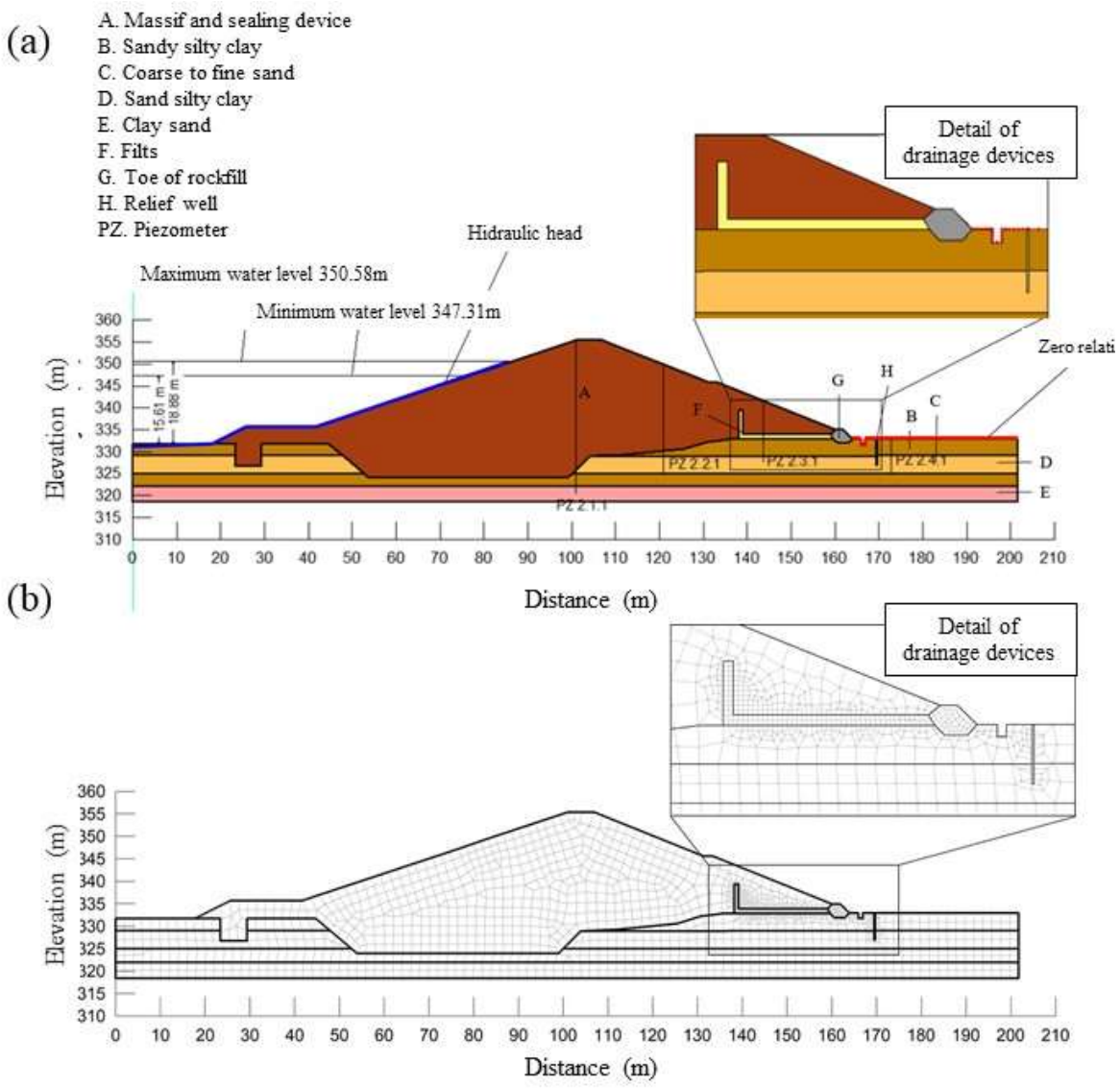

Figura 8 – Domínio do modelo 2D (a) e malha de elementos finitos (b)
Source: Authors (2023)

For each material present in the dam body and foundation, the hydrogeological property k was assigned. The initial values used at the beginning of sensitivity analysis and model calibration were the same as those presented in Table 1. As the drainage boundary condition was not used in this model, the internal drainage system and the relief well were assumed to be composed of sand with k equal to 10-2 m/s. In this model, the constituent material of the dam body was also considered homogeneous and anisotropic, while the others were homogeneous and isotropic, similar to the 3D model.

4.3 Sensitivity analysis, calibration and models validation

The sensitivity analysis and calibration of the transient 3D flow model were conducted in two stages, with the first stage considering the steady-state flow model and the second stage involving the transient model.

In the first stage, the hydrogeological property k of the constituent materials of the dam body and foundation was evaluated by varying the values individually, considering the hydraulic head in the reservoir to be 14.31 m (recorded on January 9, 2013). Simultaneously, the steady-state flow model was calibrated, minimizing the R and RMS of hydraulic

heads in the dam body and foundation by adjusting the k values within the ranges specified by Chapuis and Aubertin (2003) and/or close to those obtained in tests presented in the executive project. Finally, the water table was obtained, considered as the initial condition for the second stage of sensitivity analysis and calibration under transient conditions.

In the sensitivity analysis and calibration of the transient 3D model, the R and RMS errors of hydraulic heads in the dam body and foundation were calculated, taking as reference the instrument readings at the beginning and end of the period from January 9 to February 13, 2013, considering the corresponding hydraulic heads in the reservoir of 14.31 m and 13.94 m. Minimizing these errors resulted in the calibration of the model, involving adjustments to the hydrogeological properties SS and Sy, in addition to the conductance of the drains. The variations in the values of SS and Sy were made within the ranges specified by Germain et al. (2020) and Johnson (1967), respectively.

The validation of the transient 3D flow model was conducted for the period from January 9 to December 20, 2013, divided into seven sequences of uninterrupted simulations. Each sequence considered variable hydraulic heads in the reservoir (14.31 m on January 9, 13.88 m on February 20, 13.37 m on April 25, 12.63 m on July 12, 12.10 m on August 28, 11.39 m on December 16, and 10.79 m on December 4). The water table used as the initial condition, corresponding to January 9, was previously calculated in a steady-state simulation. At the end of each simulation sequence, the R and RMS errors of hydraulic heads in the dam body and foundation were calculated.

Regarding the 2D steady-state flow model, only the first stage was conducted. Similar to the 3D model, in the calibration of the 2D steady-state model, the goal was to minimize the average error (R) and normalized root mean square error (RMS) by adjusting the hydraulic conductivity within specified ranges. The maximum reservoir level from 2009 (recorded on May 5, 2009) was used for calibration, and the minimum level (recorded on February 18, 2009) was considered for validation**.**

4.4 Simulation of scenarios

Two scenario simulations were conducted using the 3D transient flow model. The first, covering the period from January 2 to December 31, 2009 (with hydraulic loads in the reservoir varying from 15.61 m to 18.88 m), was used to assess the performance of the internal drainage system and relief wells. The scenario simulation in the 2D flow model was employed to evaluate the functioning of the internal drainage system and relief wells, corresponding to January 2, 2009, with a hydraulic load in the reservoir of 15.61 m. On the other hand, the second simulation, from June 14 to June 28, 2022 (with variations in hydraulic loads in the reservoir from 18.30 m to 18.20 m), was employed to check the model's response to current records.

5. Results and discussion

5.1 Sensitivity analysis and calibration/validation of the 3D model

In the first stage of the sensitivity analysis and calibration of the 3D model, the results were sensitive to variations in the values of k for the sandy-silt-clay layer in the dam, the silty-sandy-clay layer in the foundation, and the layer of gravel in the riprap, with R and RMS errors of hydraulic head varying from -0.27 to -0.58 and 0.223 to 0.233, respectively. However, it did not show sensitivity to variations in the conductance of the drains.

In the second stage, the results are presented in Table 2, showing the evolutionary sequence of simulations used in the model calibration, the adjusted values of k for each material, and the smallest R and RMS errors. In the first sequence, after minimizing the errors, the adjusted k value was fixed, repeating the procedure in the following sequence and so on. Thus, there is a reduction in the absolute values of errors with the evolution of the sequences. The model was calibrated in the last sequence, with the adjusted values of k, resulting in R = -0.27 m and RMS = 0.223. After calibration, only the values corresponding to the sandy-silt-clay layer in the dam, the silty-sandy-clay layer in the foundation, the gravel in the riprap, and the gravel in the toe protection converged to the values adopted at the beginning of the process (Table 1).

Table 2 – Evolutionary sequence of simulations used in the calibration of the stationary 3D model, adjusted k values for each material, and the smallest R and RMS in each sequence.

Sequence	Material	Location	$k_{,ajust}$ (m/s)*	R (m)	RMS (-)
1	Silty-clayey-sand	Maciço	10^{-4}	-0,58	0,233
2	Silty sand	Foundation	10^{-5}	-0,51	0,231
3	Clayey sand	Foundation	10^{-6}	-0,51	0,230
4	Medium to coarse sand	Foundation	10^{-4}	-0,51	0,230
5	Fine to medium sand	Foundation	10^{-4}	-0,51	0,230
6	Fine to coarse sand	Foundation	10^{-4}	-0,51	0,230
7	Fine sand with gravel	Foundation	10^{-4}	-0,51	0,230
8	Silty sandy clay	Foundation	10^{-6}	-0,31	0,223
9	Sandy clayey silt	Foundation	10^{-5}	-0,28	0,223
10	Crushed Stone	Rip-rap	10^{-3}	-0,27	0,223
11	Crushed Stone	Rock toe	10^{-2}	-0,27	0,223

* For the dam body $k_{ajust} = k_{x11} = k_{x22}$ e $k_{x33}=10^{-1}\ k_{ajust}$;
* For the remaining layers $k_{ajust} = k_{x11} = k_{x22} = k_{x33}$.

Source: Authors (2023)

The transient 3D flow model was not sensitive to variations in the values of SS, Sy, and drain conductance, remaining the same as adopted at the beginning of the process. It was validated in seven sequences of uninterrupted simulations, with R and RMS errors of hydraulic loads ranging from -0.52 m to -0.33 m and 0.222 to 0.236, respectively (Table 3).

Table 3 – Simulation sequence and R and RMS errors used in the validation of the transient 3D flow model.

Sequence	R (m)	RMS (-)
1	-0,41	0,228
2	-0,33	0,222
3	-0,46	0,228
4	-0,37	0,236
5	-0,41	0,232
6	-0,49	0,235
7	-0,52	0,231

Source: Authors (2023)

5.2 Sensitivity analysis and calibration/validation of the 2D model

The steady-state 2D flow model was sensitive to variations in the values of k for layers of sandy-silt-clay in the embankment, layers of sandy-clay, medium to coarse sand, sandy-clayey silt, and layers of gravel in the relief well, in the toe riprap, and in the filters. Errors in R and RMS of hydraulic loads ranged from -0.10 to 0.18 and 0.73 to 0.95, respectively. The evolutionary sequence of simulations used in the calibration of the 2D steady-state model, the adjusted values of k for each material, and the lowest R and RMS errors for each sequence are shown in Table 4. The model was

calibrated with the adjusted k values, resulting in R = -0.13 m and RMS = 0.95. After calibration, none of the values converged to those adopted at the beginning of the process (Table 1), and only the value corresponding to the clayey sand in the foundation was similar to that obtained in the calibration of the 3D model (the others were lower).

Table 8 – Evolutionary sequence of simulations used in the calibration of the stationary 2D model, adjusted k values for each material, and the smallest R and RMS in each sequence.

Sequence	Material	Location	k_{ajust} (m/s)*	R (m)	RMS (-)
1	Silty-Clayey Sand	Dam body	10^{-5}	-0,10	0,73
2	Silty sand	Foundation	10^{-6}	-0,13	0,95
3	Medium to coarse sand	Foundation	10^{-6}	-0,10	0,73
4	Silty-sandy clay	Foundation	10^{-8}	0,18	0,82
5	Sandy-clayey silt	Foundation	10^{-7}	0,17	0,83
6	Crushed stone	Poço de alívio	10^{-2}	0,18	0,82
7	Crushed stone	Rock toe	10^{-3}	0,11	0,95
8	Crushed stone	Filters	10^{-3}	-0,13	0,95

* For the dam body $k_{ajust} = k_{x11} = k_{x22}$ e $k_{x33}=10^{-1}\ k_{ajust}$;
* For the remaining layers $k_{ajust} = k_{x11} = k_{x22} = k_{x33}$.

Source: Authors (2023)

5.3 Simulations

The simulation of the first scenario using the 3D transient flow model showed that the internal drainage system remained submerged throughout the period with upwellings to the downstream slope. Figure 9 depicts the flow corresponding to the maximum load (May 5, 2009) in the maximum section.

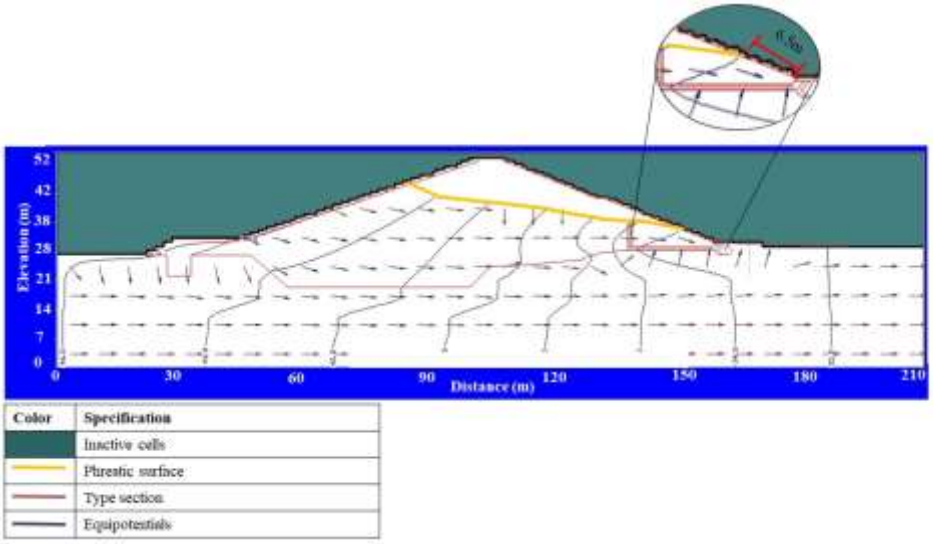

Figura 9 – Directions of the flow velocity vectors obtained in the first scenario of the three-dimensional model.
Source: Authors (2023)

The directions of the flow velocity vectors in the maximum section (Figure 9) indicate that the internal drainage system was unable to capture the entire flow from the dam and foundation. This failure is likely due to the reductions in the dimensions of the horizontal and vertical filters carried out during the construction. Similar results were also observed in all sections, but with more evidence in areas near the abutments, where part of the foundation consists of sandy layers (fine to medium sand, medium to coarse sand, and fine gravelly sand). This situation, similar to that found by Chen and Zhang (2006), suggests that the abutment boundaries are at a higher risk of rupture due to regressive erosion.

On the other hand, the stationary 2D flow model showed different results, indicating that the internal drainage system was able to capture and direct flows within the dam, protecting the downstream toe against saturation. Additionally, the relief well captured the flow from the confined layer of the foundation, reducing artesian pressures (Figure 10).

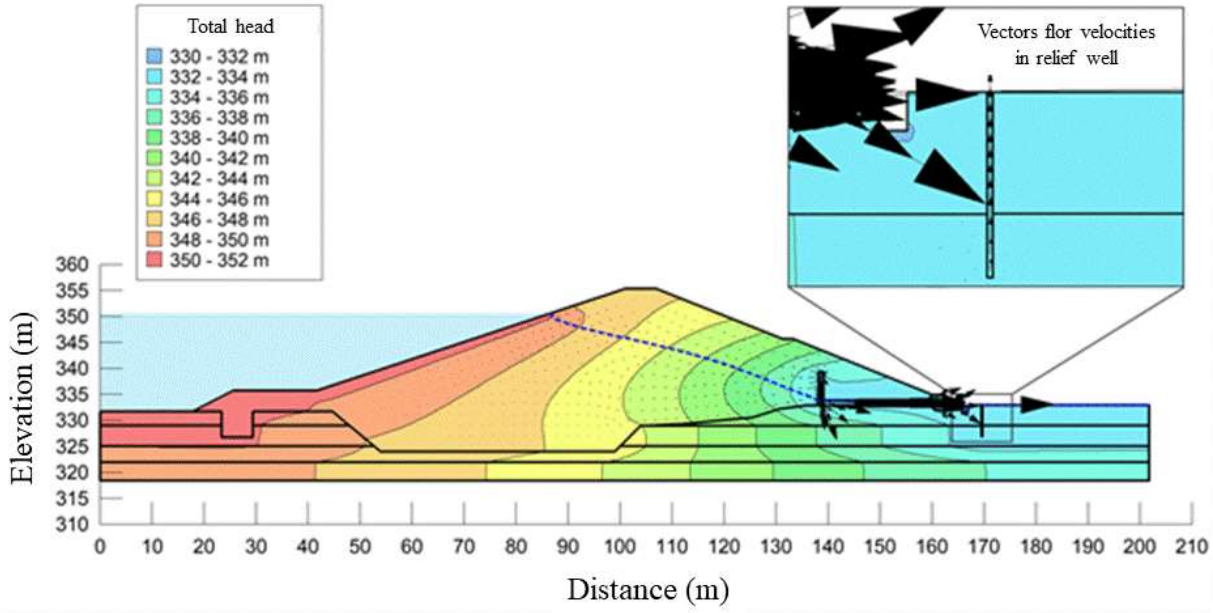

Figure 10 – Flow velocity vectors obtained through the 2D steady-state flow model.
Source: Authors (2023)

The percolation flows in the dam body and foundation obtained from the transient 3D flow model were 1.49 x 10-4 m3/s/m and 1.52 x 10-5 m3/s/m, respectively. In contrast, the stationary 2D flow model yielded percolation flows of 4.13 x 10-5 m3/s/m and 1.28 x 10-6 m3/s/m, approximately ten times smaller than those calculated in the transient 3D flow model. These results are consistent with findings by Chen and Zhand (2006), who observed that percolation flows in the dam body and foundation are higher in the 3D analysis.

This suggests that 2D stationary analysis may underestimate results, potentially leading to misguided decision-making (Nazari, 2018). In the stationary 2D model, the maximum hydraulic gradient calculated by SEEP/W in the ascending flow region downstream was 0.75 m/m (located in the upper confining layer of the foundation below the drainage ditch). This value was less than the critical hydraulic gradient of 0.84 m/m, suggesting that the upper confining layer can be considered hydraulically stable under ascending flow conditions. In a test simulation where the relief well was deactivated, an increase in hydraulic gradients in the downstream ascending flow region was observed, with values well above the critical threshold (2.31 m/m, below the drainage ditch). These results indicate that the effective operation of the relief well contributes to the hydraulic stability of the confining layer in the downstream ascending flow region of the dam.

As argued by Serafin (1985), the analysis of relief wells from the 3D model is more comprehensive, as it is possible to observe in the stratified longitudinal profile (Figure 11) that some wells are installed above the confined permeable layer, presenting conditions for artesianism to occur. This can lead to the development of high overpressures, with a potential compromise to the hydraulic stability of the foundation. This instability was observed by Oliveira (2020) when identifying

upwellings on the downstream slope of the dam, requiring the installation of a flow meter for flow monitoring (Ceará, 2018).

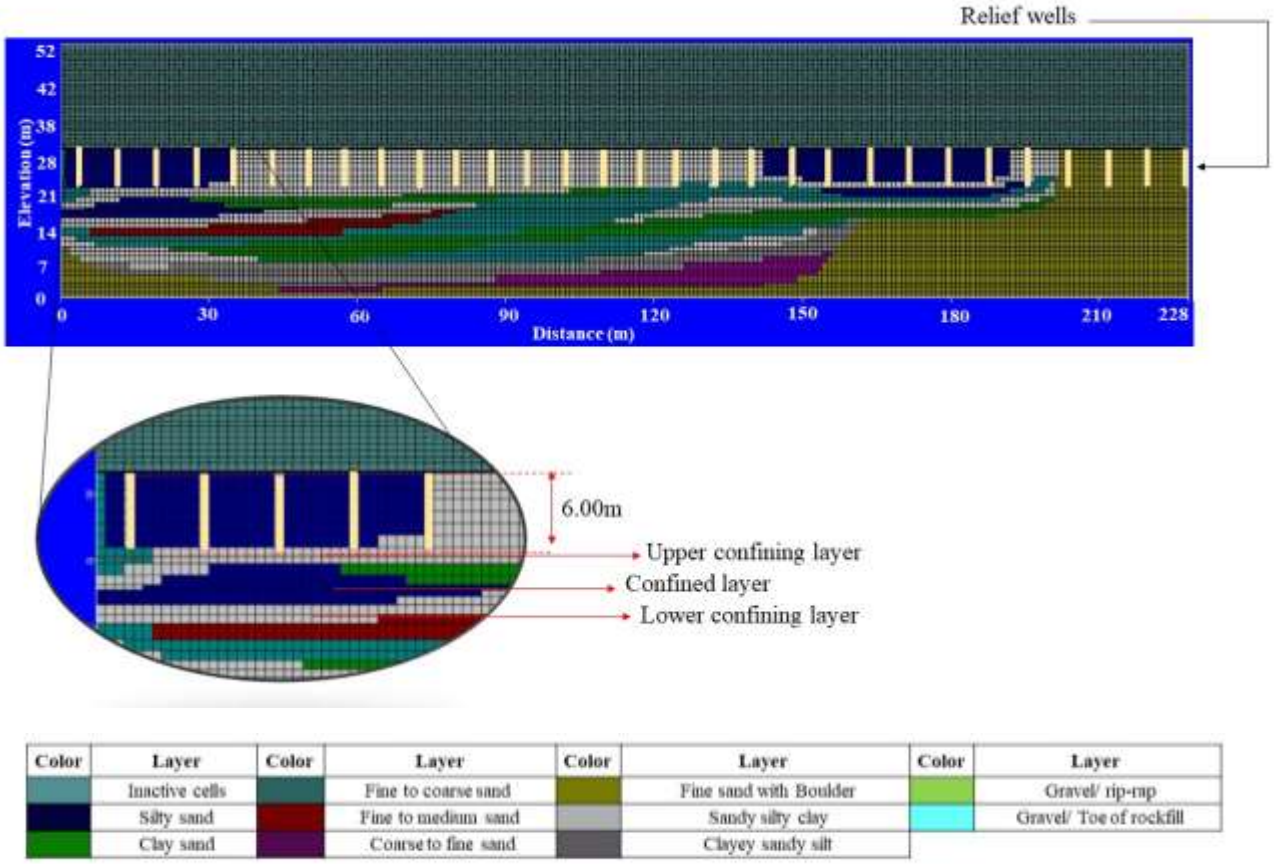

Color	Layer	Color	Layer	Color	Layer	Color	Layer
	Inactive cells		Fine to coarse sand		Fine sand with Boulder		Gravel/ rip-rap
	Silty sand		Fine to medium sand		Sandy silty clay		Gravel/ Toe of rockfill
	Clay sand		Coarse to fine sand		Clayey sandy silt		

Figure 11 – Stratified longitudinal profile discretized with the location of relief wells. Parte superior do formulário
Source: Authors (2023)

When deactivating the relief wells in the transient 3D model, it was not possible to observe changes in the seepage at the downstream slope, indicating that it possibly occurs due to alterations made in the internal drainage system during the construction. Simulations with variations in the conductance of the internal drainage system (representing a possible clogging) showed an increase in the values of R and RMS, indicating a situation that does not represent the current condition.

The simulation of the second scenario using the transient 3D flow model showed the internal drainage system submerged and an increase in the extent of the seepage, which rose to 17.0 m above the base of the downstream slope, near the right abutment (Figure 12). This situation demonstrates that through 3D modeling, it is possible to analyze the entire structure of the dam and foundation, assessing potential problems that typically originate in these regions (Chen and Zhand, 2006), providing more accurate results than 2D modeling (Zang et al., 2016).

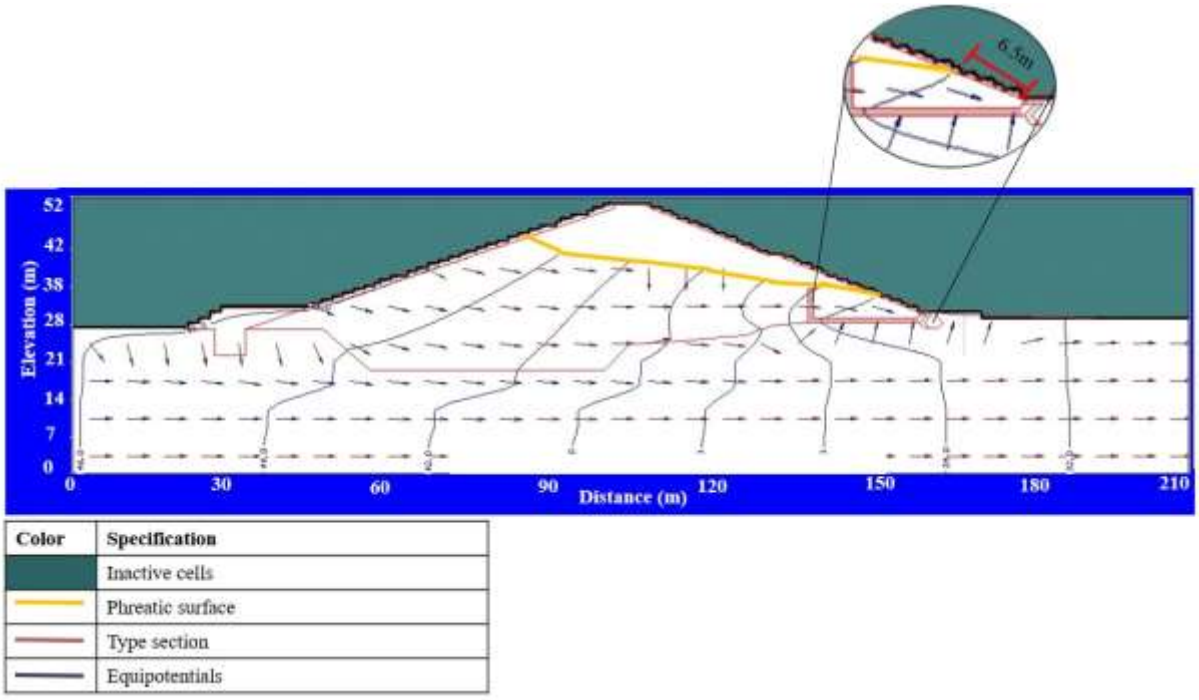

Figura 12 – Seepage on the downstream slope observed near the right abutment during the simulation of the second scenario.
Source: Authors (2023)

It is worth noting that due to the intensification of seepage on the downstream slope, in the second semester of 2022, the construction of an inverted drain was initiated. This situation, as described by Rocha et al. (2023), could have been avoided, as simulations considering extreme cases, such as accumulation over an extensive period, could suggest control over the reservoir water levels and an increase in the frequency of instrument monitoring, reducing the need for corrective measures.

6. Final Considerations

The 3D hydraulic flow modeling proved to be relevant in simulating more realistic events and obtaining more consistent results compared to 2D modeling. This is due to the fact that in 3D analysis, the entire structure is modeled, not just the maximum section as conventionally done, making it capable of predicting issues in the abutments.

Only in the 3D modeling, it was possible to assess issues observed in the field, such as the existence of faults in the internal drainage system, resulting in significant seepage in the downstream slope, and the occurrence of errors in the installation of some relief wells, contributing to the hydraulic instability of the foundation downstream.

The 3D and transient hydraulic flow modeling in the dam's dam body and foundation proved to be an important tool in analyzing the percolation dynamics, potentially contributing to decision-making in response to unforeseen events that may occur during the phases of project development, construction, and reservoir maintenance.

References

ALVES, Marina Calisto; LIMA, Filipe Augusto Xavier. The construction of dams and its effects on rural communities: an analysis from the Novo Alagamar Resettlement. *Interações*, Campo Grande, MS, v. 23, n. 2, p. 457-471, Apr./Jun. 2022.

ARAÚJO, F. R. *Geotechnical risk: a stochastic approach for the stability analysis of slopes of the Olho D'água Dam in the State of Ceará*. 2013. Dissertation (Master's in Civil Engineering) - Center for Technology, Federal University of Ceará, Fortaleza, 2013.

Bayat M, Eslamian S, Shams G, Hajiannial A (2019) The 3D analysis and estimation of transient seepage in earth dams through PLAXIS 3D software: neural network. *Environ Earth Sci* 78: 571.

BRAZIL. Presidency of the Republic. Civil House. Subsecretariat for Legal Affairs. Law No. 14,066 of September 30, 2000. Amends Law No. 12,334, of September 20, 2010, which establishes the National Dam Safety Policy (PNSB), Law No. 7,797, of July 10, 1989, which creates the National Environmental Fund (FNMA), Law No. 9,433, of January 8, 1997, which institutes the National Policy on Water Resources, and Decree-Law No. 227, of February 28, 1967 (Mining Code). Official Gazette of the Union, Sep 30, 2020.

COGERH, Companhia de Gestão dos Recursos Hídricos. Diagnosis of Instrumented Dams in the State of Ceará Monitored by COGERH. 2011.

Freeze, R.A., and Cherry, J.A. 1979. Groundwater. Prentice-Hall, Englewoods Cliffs, N.J.

GEO-SLOPE, SEEP/W for seep analysis – User's Guide. GEO-SLOPE International Ltd. Canada, 2001.

HUSSAIN, Arafat; ALI, Rashid. Numerical Approximation of One-Dimensional Transport Model Using a Hybrid Approach in Finite Volume Method", *Mathematical Problems in Engineering*, vol. 2023, 2023.

López-Acosta, N. P. , & Mendoza-Promotor, J. A. (2016). Study of Unsaturated Soils by Coupled Numerical Analyses of Water Flow-Slope Stability. In (Ed.), Groundwater - Contaminant and Resource Management. IntechOpen.

MCDONALD, M.G. E HARBAUGH, A.W. A Modular three-dimensional Finite Difference Groundwater Flow Model. In:__**USGS Techniques of Water Resources Investigations**. Washington - United States: USGS, 1988, v.6. cap.4.

MOREIRA, Aniele Lacerda; AZEVEDO, Ilana Borges de; SANTOS, Isabella Christine de Paula. Analysis of Percolation and Slope Stability in a Homogeneous Earth Dam from the Perspective of Dam Safety, In IX *Scientific Meeting of Engineering*, Rio Verde University - UniRV, 2019.

PASHAH,S. On the Use of Commercial Finite Element Packages for a Dimensionless Solution to a Class of Problems, *Computational and Mathematical Methods*, vol. 2023, 2023.

Qun Chen and L M Zhang. Three-dimensional analysis of water infiltration into the Gouhou rockfill dam using saturated-unsaturated seepage theory. *Canadian Geotechnical Journal*. 43(5): 449-461.

Nazari S, Zamani M, Moshizi SA. Comparison between two-dimensional and three-dimensional computational fluid dynamics techniques for two straight-bladed vertical-axis wind turbines in inline arrangement. *Wind Engineering*. 2018;42(6):647-664.

PIMENTA, Rafael Colombo; BACELLAR, Luís de Almeida Prado; RJEILLE, Milena Jorge; MOREIRA, Rubens Martins. State of the art on tracers applied to the evaluation of water leaks in dams. *Tchê Química Journal, v16.n31, 2020.*

ROCHA, Othon José; MARTINI FILHO, Luiz Renato; BENEVENTE, Caio Gripp; IMBUZEIRO, Letícia. CFD-3D modeling applied to the mining sector. XXXIV *National Seminar on Large Dams*, Foz do Iguaçu – PR, 2023.

SANTOS, L. L., CABRAL, J. J. S. P., CIRILO, J. A, FREITAS, D. A., SENS, M. L., ARAGÃO, R., BARROS, T. H. S.. Application of filtration technology for diffuse population in the Pernambuco Semiarid. *Brazilian Journal of Water Resources*, V. 19 n. 4, p 49-85, 2014.

SRH – Secretaria de Recursos Hídricos do Estado do Ceará. Olho D'água Dam Várzea-Alegre-Ce: executive project – general report. *Volume I*, 1988a.

SRH – Secretaria de Recursos Hídricos do Estado do Ceará. Olho D'água Dam Várzea-Alegre-Ce: executive project – geological and geotechnical report. *Volume II*, 1988b.

SRH – Secretaria de Recursos Hídricos do Estado do Ceará. Olho D'água Dam Várzea-Alegre-Ce: executive project - technical specifications. *Volume IV*, 1988c.

TERZAGHI, K.; PECK, R. B. Soil Mechanics in Engineering Practice. Translation Antônio José da Costa Nunes and Maria de Lourdes Campos Campelo. Rio de Janeiro: Ao Livro Técnico S.A.,1962.

XU, Chenyang, HUO, Zhijun. Numerical Simulation of Gravity Anomaly Based on the Unstructured Element Grid and Finite Element Method", *Mathematical Problems in Engineering*, v. 2020, 2020.

XU, Guanchao; GUO, Bowen; MENG, Zhuolun; ZHAO, Jiwei. Review of seismic safety of gravity dams based on the finite element method. Geofluids, vol. 2022, article ID 5463613, 8 pages, 2022.